Kinematics and Design of a Portable and Wearable Exoskeleton for Hand Rehabilitation

Marco Cempini, *Student Member, IEEE*, Stefano Marco Maria De Rossi, *Student Member, IEEE*, Tommaso Lenzi, *Student Member, IEEE*, Mario Cortese, Francesco Giovacchini, Nicola Vitiello, *Member, IEEE* and Maria Chiara Carrozza, *Member, IEEE*

***Abstract*— We present the kinematic design and actuation mechanics of a wearable exoskeleton for hand rehabilitation of post-stroke. Our design method is focused on achieving maximum safety, comfort and reliability in the interaction, and allowing different users to wear the device with no manual regulations. In particular, we propose a kinematic and actuation solution for the index finger flexion/extension, which leaves full movement freedom on the abduction-adduction plane. This paper presents a detailed kineto-static analysis of the system and a first prototype of the device.**

I. INTRODUCTION

The field of rehabilitation robotics gained momentum in last years [1] thanks to its potential applications in the treatment of neuro-muscular impairments following, e.g., stroke, spinal cord injuries (SCI) and cerebral palsy [2]. Usage of robotic devices for the physical treatment allows repetitive and long-duration therapy sessions, with minimal effort and maximum repeatability, and ensures a quantitative evaluation of the treatment's outcome. In this work, we focus on hand function restoration, a critical upper limb rehabilitation following widespread disorders such as stroke and SCI [3].

Two are the robot approach toward rehabilitation: end-point machines [4], [5] and exoskeletons [6], [7]. The former are typically easier to control and install, and show a good mechanical solidity, having only one point of interaction with the subject (e.g. the hand). However they do not allow to control limb posture and to measure the position of each body joint [8]. Wearable exoskeletons overcome these problems by targeting directly each human joint, but conversely they have greater mechanical complexity, and face strict requirements for weight and encumbrance, given the close interaction with the user.

Approaching the human hand rehabilitation is very challenging: its structure offers a very limited space for physical interaction with external devices. Solutions following end-point approach [9]-[12], in which the robot exchanges forces at the fingertip, lead to simple actuation and control systems, but prevent to control the movement of each joint. Multi-phalanx strategies lead to more complex and bulky platforms, whose effectiveness is improved at the expense of portability [13].

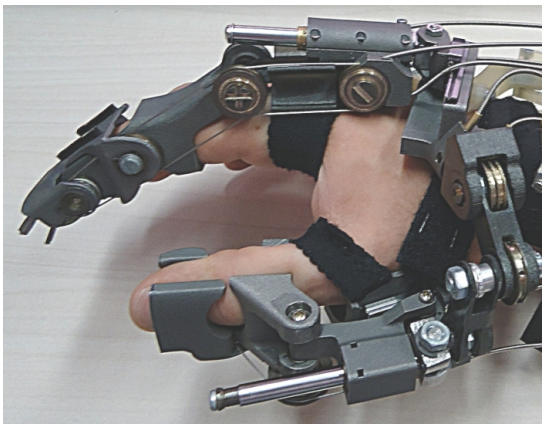

FIG. 1: Hand exoskeleton prototype (patent pending [25]), composed by index, thumb, wrist, forearm fitting and remote actuation modules. The present paper deals with the design of the index module.

Many examples of multi-phalanx exoskeletons can be found in haptic [14], where they act as measurement devices and are actuated to simulate the virtual-reality environment interaction. These robots are typically not portable given their complex sensory and actuation system, and cannot generate the high forces required by rehabilitation therapies.

Some examples of wearable robots for hand rehabilitation can be found as well [15]-[20]. The review of these devices points out two major critical aspects of robots for hand rehabilitation: *wearability* and *adaptability*. The first aspect relates with the need of developing a lightweight structure and a portable actuation system capable of generating the forces required by the treatment. The second aspect requires the robot to adapt to different users, who have different hand size, different disorders and require specific rehabilitation protocols. *Variability* of the hand kinematics is also critical: bone morphology, tissues deformations and inter- and intra-subject variations complicate the development of a robot which can be *adaptable* and *compliant* to this variables. A typical problem faced in the literature is that of *human-robot axes misalignment* [21]-[23], which if not addressed introduces undesired effects on the muscle-skeletal structure.

In this work, we present the design of a new exoskeleton for the rehabilitation of the flexion/extension (f/e) movement of

This work was supported in part by the European Union within the WAY project FP7/2007-2013 under GA 288551; Regione Toscana under the Health Regional Research Programme 2009 within the EARLYREHAB project; and the Italian Ministry of Economic Development within the AMULOS project, work programme Industria 2015, under GA MI01_00319. Authors are with The BioRobotics Institute, Scuola Superiore di Studi Universitari e di Perfezionamento Sant'Anna, viale Rinaldo Piaggio, 34, 56025, Pontedera, Pisa, Italy. Marco Cempini is corresponding author; phone: +39 050 883475, fax: +39 050 883497, e-mail m.cempini at sssup.it

978-1-4673-6024-1/13/$31.00 ©2013 IEEE

the fingers (see Fig. 1), one of the most critical capabilities to recover in neuro-rehabilitation treatments of the hand [24]. We show how improved wearability and adaptability requirements were faced and solved in the mechanical design, which features misalignment-free kinematics, effective torque transmission to inter-phalangeal joints, light weight and high portability [25]. In particular we will focus on the full kinematic and actuation design and their implementation on the index finger module of the exoskeleton.

II. SYSTEM REQUIREMENTS

The system requirements were chosen to render *portability* and *adaptability* in quantitative design criteria and trying to match them with a light and low-encumbrance wearable structure. Fig. 1 gives a global view of the hand exoskeleton system, with its index and thumb module. The present paper focuses on the design for the index f/e motion of its articulations: metacarpo-phalangeal (MCP), proximal-interphalangeal (PIP) and distal-interphalangeal (DIP), modelled as revolute joints, [26]. To ensure maximum wearability, the device also allows for a passive movement on the abduction-adduction plane.

A. Bowden-cable under-actuation system

Placement of the actuators is critical for the usability of the device. If the motors are near the active axes the transmission is simpler, more reliable and efficient, but inertia and overall dimension increase (e.g. [9], [19]). On the contrary, if the actuation system is remote [17], [18], [20], [27], [28] the transmission system will likely be heavier (e.g. bearing units, leverages [10]).

To reduce the weight of the device on the hand, we decided to implement a remote actuation system using a compliant transmission based on Bowden-cables (see Fig. 1) [29]. This solution has been already tested in [20] and, apart from an efficiency factor that must be taken into account for friction losses in the hose, it has been shown to be a reliable trade-off between precision-bandwidth and encumbrance-complexity requirements.

Cable driving is a convenient solution for underactuated systems, since one cable can travel through multiple pulleys and drive several joints. Underactuated solutions [30] reduce the complexity, the number of motors, and still can allow an anthropomorphic kinematic behaviour. To achieve underactuation, the routing pulleys must be idle, so that the cable tension can be transmitted to the moving parts independently from the finger posture.

B. MCP joint self-alignment

A key feature of our platform is the presence of a self-aligning mechanism ([21]) for the MCP finger joint. This bypasses the human MCP joint with a parallel chain, attached on top the user's hand dorsum to the first phalanx.

The problem of misalignment is extremely important for the MCP joint. In fact, not only the MCP axis is hardly localizable in vivo, but also translates and rotates greatly during the finger movement. Moreover, while all the other hand joints have an all-around physical access, the MCP of medium and ring finger is partially hidden by the rest of the hand, so that it is not possible to place a robotic linkage directly aligned to the MCP axis.

To overcome this issue we designed a novel alignment mechanism that can cope with the displacement of the MCP and with the finger's abduction-adduction, allowing to transfer the desired torque on the f/e axes only.

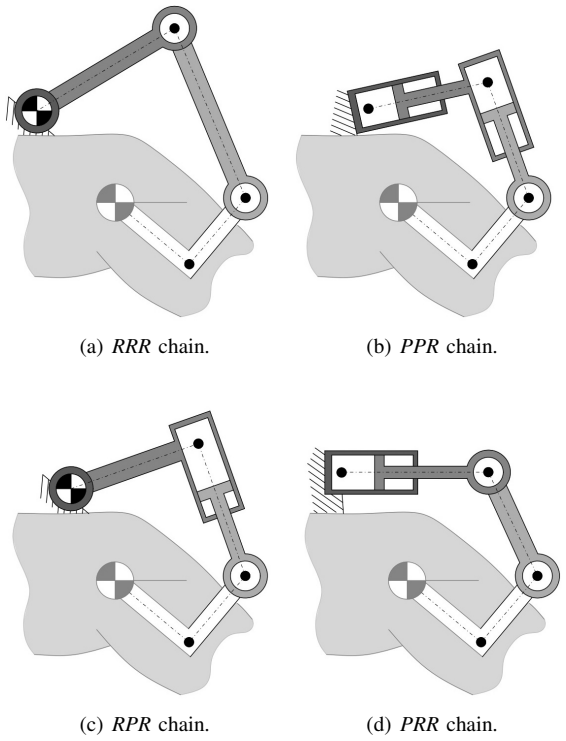

(a) *RRR* chain. (b) *PPR* chain.

(c) *RPR* chain. (d) *PRR* chain.

FIG. 2: The four possible architectures for the MCP joint mechanism. Each of the solutions ends with a revolute joint.

III. SYSTEM DESIGN

The starting point is the choice of the kinematic chain to be employed. We first focuse on the design on the f/e plane mechanism, which has strict actuation and workspace limitations, and then describe the passive mechanism for the abduction-adduction plane of motion. After the kinematic design, actuation and transmission will be presented along with a proof of its efficiency in transferring loads to the phalangeal joints.

A. Kinematics

1) MCP mechanism kinematics: The MCP mechanism forms a closed chain with the MCP human joint. The robot must then provide 3 additional DOFs between the hand dorsum and the phalanx, so that the mobility formula for a planar mechanism gives (n is the number of links, j the number of joints, f_i the number of DOFs the i-th joint) provides:

$$M = 3(n-1-j) + \sum_{i=1}^{j} f_i = 3(4-1-4) + 4 \cdot 1 = 1.$$

Since we are designing an underactuated system, the last joint of the mechanism should be an active revolute joint.

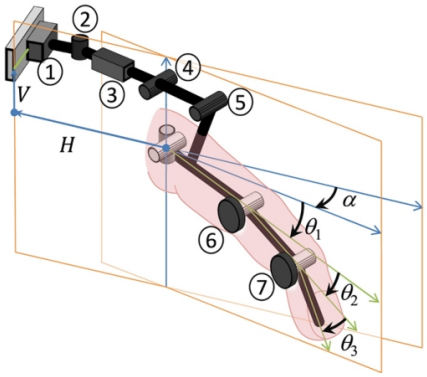

FIG. 3: Full kinematic diagram of the coupled finger-exoskeleton system. α is the abduction angle, while θ_i are the flexion ones. The plane π_{flex} is drawn with and without abduction. Numbers 1-7 are the exoskeleton joints.

This comes from the choice of using the same cable to actuate the finger's f/e joints that follow the MCP one (PIP and DIP). The mechanism can therefore assume any of the following chain structuress *RRR*, *PPR*, *RPR* and *PRR*[1], shown in Figg. 2(a)-2(d). Focusing on workspace requirements, we can draw the following conclusions:

- The trajectory of the robot links should intersect the area occupied by the hand, in the whole f/e range of motion ($\theta_1 \in [0, \frac{\pi}{2}]$).
- *RRR* has already been used in several hand exoskeleton, [16]-[27] but needs very long first and second link to avoid collision with the hand.
- *PPR* imposes workspace limitations due to the prismatic joints (e.g., it is very unlikely that the one pictured in 2(b) will permit the human joint to flex further). Their slider elements will necessary be longer than the required stroke: their direction and orientation should minimize the requested stroke and to keep the slider surplus "away" from the user hand.
- Among *RPR* and *PRR* structures, the second one seems to suffer less of the aforementioned problems, mainly because the first link of *RPR* is asked to avoid the hand space, as happens for *RRR*. Moreover, the *PRR*'s prismatic joint is more easily manageable in term of encumbrance, while the *RPR*'s prismatic slider will move around the workspace area.

Our mechanism exploits the fourth structure *PRR*: in addition to the aforementioned reasons, this choice becomes extremely convenient when extended to the abduction-adduction motion (see section III-A.3.b). It is worth to note that this choice depends greatly on the workspace required to the MCP finger joint, $\theta_1 \in [0, \frac{\pi}{2}]$: if such workspace changes, the optimal architecture may be different.

2) Multiphalangeal kinematics: The remaining joints are implemented via revolute DOFs aligned along the PIP and DIP axes. Alignment issues for such joints have not been considered directly, since such articulation are much more accessible and easier to identify than the MCP. However, in order to comply with their variability, a soft cover in Neoprene between the exoskeleton links and the phalanges is inserted: this layer absorbs potential small errors in device positioning without complicating the design. Moreover, to adapt the device to different hand size, the middle phalanx can be adjusted in length (it's splitted in two valves coupled with a dovetail in the dorsal side), and the last one has a open end, allowing the fingertip exiting from it. All the revolute joints are equipped with an idle pulley for the routing of cable actuation. The full kinematic chain employs a *PRRRR* structure, with the first actuated joints *RR* devoted to the MCP assistance, the third and the fourth *R* to PIP and DIP respectively.

The phalangeal links have a shell structure with a wide area of interaction with the finger's skin. Inter-subject differences in phalangeal length are handled by the exoskeleton design, in the following manner: the MCP mechanism allows a correct kinematic coupling even when the MCP center translates, which is equivalent to a different phalanx length; the middle phalanx links possesses an adjustable dovetail coupling that has to be matched with the user finger dimensions; the last link has an open distal end, so that the third phalanx length is not relevant.

It is worth to note how the bearing structure on the second and last phalanges is completely external (no joint or frame is present on the internal side of the finger), in order to not interfere with the middle finger when the hand closes. In fact, fingers flexion anatomically occurs with close contact between fingers inner sides, and this is a typical limitation for state-of-the-art platform which exploit direct human joints placing, like in [20] and [17].

3) Full Kinematics:

a) Flexion-extension motion: Fig. 3 shows a full schematic of the system composed by the human finger and the exoskeleton. The f/e plane π_{flex} is highlighted. Let us start the analysis from Fig. 4(b), which represents a projection of the mechanism on the π_{flex} plane, and let us take the reference position of the human joint centre as the origin, O: in addition to the MCP joint variables θ_1, we describe the misalignment effect as two unpredictable and uncontrollable MCP centre displacements from O, δ_x and δ_y. The closed kinematics of the *PRRR* mechanism is solved by (c_i and s_i are short notation for $\cos q_i$ and $\sin q_i$ respectively)

$$\begin{cases} q_3 + l_3 + l_4 c_4 + l_5 c_{45} = X_0 + \delta_x + l_h \cos\theta_1 \\ -l_4 s_4 - l_5 s_{45} = -Y_0 + \delta_y - l_h \sin\theta_1 \\ q_4 + q_5 - \frac{\pi}{2} = \theta_1 \end{cases} \Rightarrow$$

$$\Rightarrow \begin{cases} \delta_x = (q_3 - X_0) + l_3 + l_4 c_4 + l_5 c_{45} - l_h s_{45} \\ \delta_y = Y_0 - l_4 s_4 - l_5 s_{45} + l_h c_{45} \\ \theta_1 = q_4 + q_5 - \frac{\pi}{2} \end{cases}, \quad (1)$$

where X_0 and Y_0 are offset variables related to the P joint's fixed frame position. The relations between the PIP and DIP joint angles and the related exoskeleton angles are trivial,

$$\theta_2 = q_6, \theta_3 = q_7. \quad (2)$$

[1] R and P stand for revolute and prismatic joints, respectively.

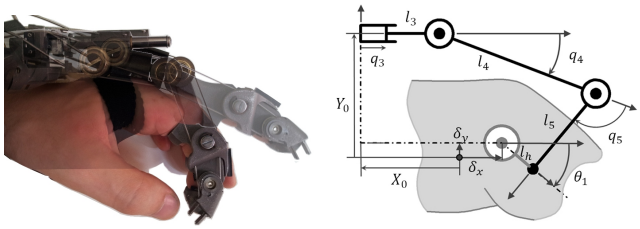

(a) (b)

FIG. 4: Flexion-extension kinematics for the MCP joint. (a): shaded view of the prototype with different flexion postures at MCP joint. (b): this draw corresponds to the side view of 3, projected on the π_{flex} plane. Joints 3-5 are involved and represented. The MCP joint centre is supposed to misplace from the reference position of the quantities δ_x and δ_y.

b) Abduction-adduction motion: Fig. 5(b) shows how the X_0 offset on the π_{flex} plane depends on the abduction angle α and on the third misalignment displacement δ_z, normal to the π_{flex} plane. This is not a drawback, but has been deliberately implemented in the design. The passive P joint of the MCP mechanism is orthogonal to both the MCP abduction-adduction and f/e axes, meaning that it can compensate for misalignments in both the motion's planes of the MCP joint. This choice drastically reduces the bulk of the exoskeleton without affecting its kinematic compatibility performances. Regarding the α contribute to X_0, simple trigonometric relations give

$$\cos\alpha(l_2+X_0(\alpha)) = l_2 + X_0|_{\alpha,\delta_z=0}\,. \tag{3}$$

Since for null abduction X_0 can be obtained from the exoskeleton fixed frame back distance H,

$$l_1 + l_2 + X_0|_{\alpha,\delta_z=0} = H,$$

equation (3) becomes

$$X_0(\alpha) = \frac{H-l_1}{\cos\alpha} - l_2. \tag{4}$$

Then, taking into account the δ_z effect we can infer

$$X_0(\alpha,\delta_z) = X_0(\alpha) - \delta_z\tan\alpha = \frac{H-l_1-\delta_z\sin\alpha}{\cos\alpha} - l_2. \tag{5}$$

From Fig. 5(b) we can also obtain the relations between q_1 and q_2 and the abduction-adduction variables:

$$\begin{cases} q_1 = -\delta_z\cos\alpha + (l_2+X_0)\sin\alpha, \\ q_2 = \alpha. \end{cases} \Rightarrow \begin{cases} \delta_z = (H-l_1)s_2 - q_1c_2, \\ \alpha = q_2 \end{cases} \tag{6}$$

Substituting (6) into (5), and putting the result into the first part of (1) δ_x can be expressed as a function of the exoskeleton variables: the complete result of the kinematic is (Y_0 has been replaced by V, the exoskeleton fixed frame vertical height)

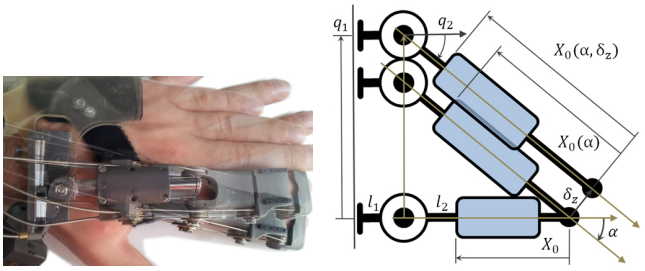

(a) (b)

FIG. 5: Abduction-adduction kinematics. (a): shaded view of the prototype with different abduction postures. (b): this draw corresponds to the top view of 3. Joints 1-3 are involved and represented: the blue box represents the top view of the mechanism of 4(b), connecting the reference frame of the q_3 slider with the MCP joint centre. In the figure, this undergoes a misplacement δ_z perpendicular to the π_{flex} plane.

$$\begin{bmatrix} \theta_1 \\ \theta_2 \\ \theta_3 \\ \alpha \\ \delta_x \\ \delta_y \\ \delta_z \end{bmatrix} = f(\mathbf{q}) \Leftrightarrow \begin{cases} \theta_1 = q_4 + q_5 - \frac{\pi}{2} \\ \theta_2 = q_6 \\ \theta_3 = q_7 \\ \alpha = q_2 \\ \delta_x = q_3 - q_1s_2 - (H-l_1)c_2 + \dots \\ \dots l_2 + l_3 + l_4c_4 + l_5c_{45} - l_hs_{45} \\ \delta_y = V - l_4s_4 - l_5s_{45} + l_hc_{45} \\ \delta_z = (H-l_1)s_2 - q_1c_2 \end{cases} \tag{7}$$

4) Workspace: Fig. 6 shows the reachable workspace for the MCP centre misalignments, with measures and prismatic joints strokes as listed in Table I. Such workspace is defined by the $(\delta_x,\delta_y,\delta_z)$ points that, for any given abduction angle $\alpha\in[0,20°]$ and flexion angle $\theta_1\in[0,90°]$, are reachable within the exoskeleton joints strokes limitations. The workspace contains a sphere of radius 5 mm centred in $\delta_{x,y,z}=0$, so that the mechanism can compensate any $\pm$5mm misalignments around the reference configuration.

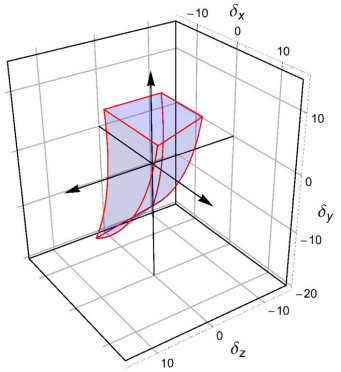

FIG. 6: Misalignments workspace: set of $(\delta_x,\delta_y,\delta_z)$ points that are reachable within the joint stroke mechanical stops for any $\alpha\in[0,20°]$ and any $\theta_1\in[0,90°]$. The workspace variables are expressed in mm.

B. Actuation and Transmission

1) Torque Transmission on the MCP joint: In this paragraph, we show how torques are transferred by our mechanism to the MCP joint. Applying the virtual work principle to (1) we can write the relation between the exoskeleton torques and the human joint ones by transposition of the Jacobian

Hand related dimensions (approx.)	H	60 mm
	V	21 mm
	l_h	5 mm
Links lengths	l_1	6.5 mm
	l_2	6.0 mm
	l_3	15 mm
	l_4	38 mm
	l_5	9 mm
Joint strokes	q_1	$-5 \div 25$ mm
	q_2	$-90 \div 90$ deg
	q_3	$-5 \div 25$ mm
	q_4	$-10 \div 90$ deg
	q_5	$-90 \div 90$ deg

TABLE I: Exoskeleton's dimensions and strokes

matrix:

$$\begin{bmatrix}\dot{\delta}_x\\ \dot{\delta}_y\\ \dot{\theta}\end{bmatrix}=\begin{bmatrix}1 & l_4s_4-l_5s_{45}-l_hc_{45} & -l_5s_{45}-l_hc_{45}\\ 0 & -l_4c_4-l_5c_{45}-l_hs_{45} & -l_5c_{45}-l_hs_{45}\\ 0 & 1 & 1\end{bmatrix}\begin{bmatrix}\dot{q}_3\\ \dot{q}_4\\ \dot{q}_5\end{bmatrix}\Rightarrow$$

$$\begin{bmatrix}\tau_3\\ \tau_4\\ \tau_5\end{bmatrix}=\begin{bmatrix}1 & 0 & 0\\ l_4s_4-l_5s_{45}-l_hc_{45} & -l_4c_4-l_5c_{45}-l_hs_{45} & 1\\ -l_5s_{45}-l_hc_{45} & -l_5c_{45}-l_hs_{45} & 1\end{bmatrix}\begin{bmatrix}F_x\\ F_y\\ T_{\theta 1}\end{bmatrix}. \quad (8)$$

where $T_{\theta 1}$ is the desired torque along the MCP axis. A reasonable actuation requirement is to keep a null F_x, F_y value in order not to burden the MCP articulation with translational forces. This requirement leads to

$$\tau_3 = 0, \tau_4 = \tau_5 = T_{\theta 1}. \quad (9)$$

As a result, the prismatic joint needs to be passive, and the revolute joints should be actuated by the same torque. This latter condition is easily implementable by means of a cable-driven underactuation: as depicted in Fig. 7, the exoskeleton's first two revolute joints are driven by a cable passing two pulleys, the first of those being idle while the second fixed with its link; pulleys radii are both R_0. Balance between input and resistant powers when the cable travel of a segment δx under a tension force T_1 leads to

$$W_{in} = T_1\,\delta x = T_1 R_0(\delta q_4 + \delta q_5) = T_1 R_0 \delta\theta_1 = W_{out} = T_{\theta 1}\delta\theta_1 \Rightarrow T_1 R_0 = T_{\theta 1}, \quad (10)$$

so that the torque on the MCP joint can be controlled by the cable's tension.

2) Mechanical implementation: In the proposed prototype two underactuation units are used: the first travels through the first two $\underline{R}$ joints, as shown in Fig. 8, and regulates the torque exerted on the MCP joint, as in equation (10). The related cables travel on the inner side of the exoskeleton. The second passes through the first three $\underline{R}$ joints via idle pulleys, and then through a fourth pulley, which is fixed to the distal link, but on the outer side of the exoskeleton (visible in Fig. 1). Fig. 8 shows a schematic of the force transmission between the various mechanic elements of the P-DIP underactuation unit: if two consecutive pulleys have different radii, the cable tension between them has a net arm with respect to the direction joining the two axes, thus exerting a torque on the corresponding link. Since the first three pulleys on the route have the same radii R_1, the cable exerts torques only on the middle and distal phalanges, without affecting the proximal one. Thus, the net torques applied to the PIP and DIP joints respectively are

$$T_{\theta 2} = T_2(R_1 - R_2), T_{\theta 3} = T_2 R_2. \quad (11)$$

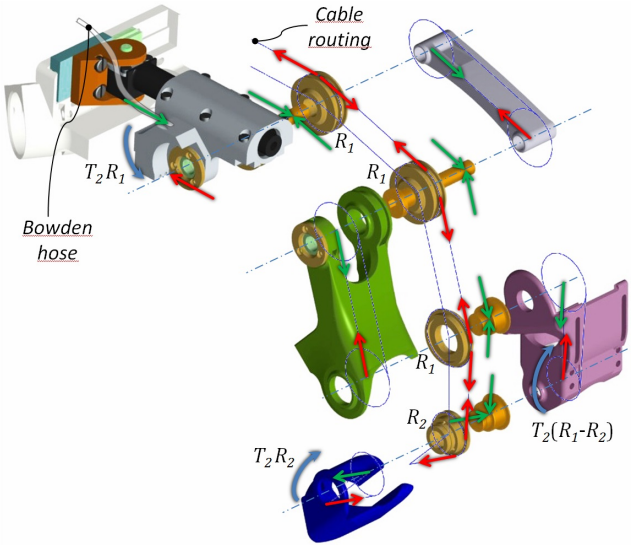

FIG. 8: Underactuation schematic. The cable exchanges a tension force T_2 with each of the pulleys and with the distal phalanx (to which its end is attached). Each component is subjected to active (red) and reaction (green)forces: the support shaft of each pulley has been drawn since it also constitutes the connecting joint. Starting from the distal extremity, we can describe the mechanics as a series of sub-assemblies (link+pulley+shaft), each of them being supported by the previous link. $R_{1,2}$ are the pulleys radii: when two consecutive pulleys have different radii, the interposed link needs a torque in order to satisfy equilibrium: such torque comes from interaction with the user's finger. The most proximal link closes the chain of forces through the Bowden sheath, loading the prismatic joint with a counter-wise torque T_2R_1.

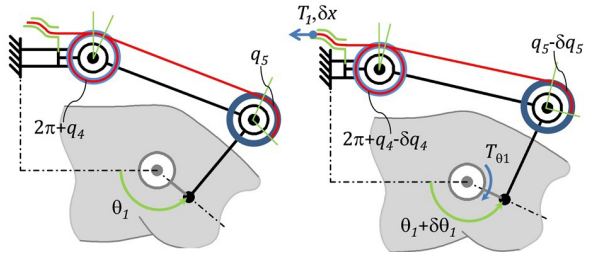

FIG. 7: Transmission of the MCP torque via underactuated pulleys. Since the straight segments have constant lenght, the cable displacement is related to the variation of the revolute joints angles, whose pulleys have radius R_0. The active work $T_1\,\delta x$ corresponds to the resistant one $T_{\theta 1}\delta\theta_1$, so that relation (10) holds.

C. Prototype

A full actuated prototype was designed and manufactured in order to test our approach and the kinematic compatibility performance, with an eye on ergonomy (Fig. 1). The exoskeleton back is split into two valves, which can be adapted to different shapes of hand dorsum. The second prismatic joint has been replaced by a cylindrical one, in order to have an additional degree of adaptability if differences in the mutual orientations of the finger and of the hand palm are present. The total weight of the device (including the thumb module, which has not be discussed here) is 500 grams. The actuation unit is remoted also beacues of its weight, around 1 kg: it encloses multiple identical transmission lines, each

	Motor	Gearhead	Spur gears	Leadscrew	Cable	Joints:	MCP-PIP-DIP
Torque Velocity	3.2 mNm 10′000 RPM	14:1	12:10	Pitch: 0.7 mm/rev Torque/axial force: 0.78 mNm/N	83 N 5.8 mm/s	$R_0 = 7$ mm $R_1 = 7$ mm $R_2 = 3.5$ mm	$0.5 - 0.25 - 0.25$ Nm $47 - 31 - 31$ deg/s

TABLE II: Prototype actuation performances

with a single motor (1331T006SR, 3.11W, Faulhaber®(D)) driving a pair of parallel leadscrews, whose nuts move the cables' tip in opposite direction, thus providing a net torque on the joints. Actuation also includes a cable pretension system, in order not to loose the pushing one: in other words, $T_{1,2}$ represents the *difference* between the tensions in the pulling and pushing cables pair. Performances are in Tab. II.

IV. CONCLUSIONS

In this paper the design of a wearable robotic device for the hand rehabilitation has been presented. The proposed conceptual architecture achieves a full kinematic compatibility through a custom mechanism that can compensate for misalignments of the MCP joint centre as well as abduction-adduction motions. The same mechanism gives the exoskeleton the possibility to fit users with different anthropometry. A remote Bowden-cable transmission was used, leading to reduced weight and bulk on the user hand. Cable transmission allows also underactuation strategies, and increased the flexibility and usability of the actuation block. Two actuators are employed: the first regulates the MCP joint net torque, which by proper choice of the travelled pulleys' radii, is transmitted avoiding undesired translational forces on user's articulation, which may negatively affect the treatment, [21], [23]. The second actuator controls the sum of PIP and DIP ones: their proportion is adjusted by the ratio R_2/R_1. Finally, a prototype of the device has been realized in order to verify the mechanical feasibility of the proposed mechanism. This new prototype shows an improved wearability and kinematic adaptability, and will be tested in order to verify how its effective performance differs from those depicted in Tab. II.

REFERENCES

[1] Krebs, H. *et al.*, "A paradigm shift for rehabilitation robotics", IEEE Eng. in Med. and Biol. Magazine, vol.27, no.4, pp.61-70, 2008.

[2] Kwakkel, G. *et al.*., "Effects of robot-assisted therapy on upper limb recovery after stroke: a systematic review", Neurorehab. and neur. repair, vol.22, no.2, pp.111-121, 2008.

[3] Takahashi, C.D. *et al.*, "Robot-based hand motor therapy after stroke", Brain, vol.13, no.2, pp.425-37, 2008.

[4] Hogan, N. *et al.*, "MIT-MANUS: a workstation for manual therapy and training", IEEE Int. Workshop on Robot and Human Communication, pp.161-165, 1992.

[5] Lum, P.S. *et al.*, "MIME robotic device for upper-limb neurorehabilitation in subacute stroke subjects: A follow-up study", J. Rehab. Res. and Devel., vol.43, no.5, pp.631-42, 2006.

[6] Pons, J.L., "Rehabilitation exoskeletal robotics. The promise of an emerging field", IEEE Eng. in Med. and Biol. Magazine, vol.29, no.3, pp.57-63, 2010.

[7] Herr, H., "Exoskeletons and orthoses: classification, design challenges and future directions", J. Neuroeng. and Rehab., vol.6, p.21, 2009.

[8] Lum, P.S. *et al.*, "Gains in upper extremity function after stroke via recovery or compensation: Potential differential effects on amount of real-world limb use", Topics in Stroke Rehab., vol.16, no.4, pp.237-253, 2009.

[9] Iqbal, J. *et al.*, "A Human Hand Compatible Optimised Exoskeleton System", 2010 IEEE Int. Conf. Rob. and Biomimetics, pp.685-690, 2010.

[10] Fontana, M. *et al.*, "Mechanical design of a novel Hand Exoskeleton for accurate force displaying", 2009 IEEE Int. Conf. Rob. Aut., pp.1704-1709, 2009.

[11] Bouzit, M. *et al.*, "The Rutgers Master II-new design force-feedback glove", IEEE/ASME Tran. Mech., vol.7, no.2, pp.256-263, 2002.

[12] Brokaw, E.B. *et al.*, "Hand Spring Operated Movement Enhancer (HandSOME)", IEEE Trans. Neur. Sys. and Rehab. Eng., vol.9, no.4, pp.391-399, 2011

[13] Huang, Y.Y. and Low, K.H., "Initial analysis and design of an assistive rehabilitation hand device with free loading and fingers motion visible to subjects", 2008 IEEE Int. Conf. Systems, Man and Cybernetics, pp.2584-2590, 2008.

[14] Blake, J. and Gurocak, H.B., "Haptic Glove With MR Brakes for Virtual Reality", IEEE/ASME Trans. Mech., no.5, pp.606-615, 2009.

[15] Choi, B.H. and Choi, H.R., "SKK Hand Master-hand exoskeleton driven by ultrasonic motors", 2000 IEEE/RSJ Int. Conf. Int. Robots and Systems, pp.1131-1136, 2000.

[16] Lucas, L. *et al.*, "An EMG-Controlled Hand Exoskeleton for Natural Pinching", J. of Rob. and Mech., 2004.

[17] Wege, A. *et al.*, "Mechanical design and motion control of a hand exoskeleton for rehabilitation", 2005 IEEE Trans. Mech., pp.155-159, 2013.

[18] Jones, C. *et al.*, "An Actuated Finger Exoskeleton for Hand Rehabilitation Following Stroke", 2007 IEEE Int. Conf. Rehab. Rob., pp.896-901, 2007.

[19] Hasegawa, Y. *et al.*, "Five-fingered assistive hand with mechanical compliance of human finger", 2008 IEEE Int. Conf. Rob. Autom., pp.718-724, 2008.

[20] Chiri, A. *et al.*, "Mechatronic Design and Characterization of the Index Finger Module of a Hand Exoskeleton for Post-stroke Rehabilitation", IEEE/ASME Trans. Mech., vol. 17, no.5, pp.884-894, 2012.

[21] Stienen, A.H.A. *et al.*, "Self-aligning exoskeleton axes through decoupling of joint rotations and translations", IEEE Trans. Rob., vol.25, no.3, pp.628-633, 2009.

[22] Vitiello, N. *et al.*, "NEUROExos: a Powered Elbow Exoskeleton for Physical Rehabilitation", IEEE Trans. Rob., vol.29, no.1, pp.220-235, 2013.

[23] Cempini, M. *et al.*, "Self-Alignment Mechanisms for Assistive Wearable Robots: a Kineto-Static Compatibility Method", IEEE Trans. Rob., vol.29, no.1, pp.236-250, 2013.

[24] DeLisa, J.A. and Gans, B.M., "Physical Medicine & Rehabilitation: Principles and Practice", ed. Lippincott Williams & Wilkins, 2005.

[25] M. Cempini *et al.*, "Dispositivo indossabile per la riabilitazione della mano", Brevetto di Invenzione Industriale (Italian Patent) num. PI2012A000094, application date August 28, 2012.

[26] Chao, E.Y.S. *et al.*, "Biomechanics of the Hand: a basic research study", book available at `http://www.worldscibooks.com/lifesci/0321.html`.

[27] Zheng, R. and Li, J., "Kinematics and Workspace Analysis of an Exoskeleton for Thumb and Index Finger Rehabilitation", 2010 IEEE Int. Conf. Rob. and Biomimetics, pp.80-84, 2010.

[28] Wang, J. *et al.*, "Design of an exoskeleton for index finger rehabilitation", 2009 IEEE Int. Conf. Eng. in Med. and Biol. Society, pp.5957-5960, 2009.

[29] Veneman, J.F. *et al.*, "A Series Elastic- and Bowden-Cable-Based Actuation System for Use as Torque Actuator in Exoskeleton-Type Robots", Int. J. Rob. Res., vol.25, no.3, pp.261-281, 2006.

[30] Birglen, L. and Gosselin, C.M., "Kinetostatic Analysis of Underactuated Fingers", IEEE Trans. Rob. Aut., vol.20, no.2, pp.211-221, 2004.